

# Controlling the Supramolecular Assembly of Redox-Active Dendrimers at Molecular Printboards by Scanning Electrochemical Microscopy

Christian A. Nijhuis,<sup>†</sup> Jatin K. Sinha,<sup>‡</sup> Gunther Wittstock,<sup>\*,‡</sup> Jurriaan Huskens,<sup>†</sup>  
Bart Jan Ravoo,<sup>\*,‡</sup> and David N. Reinhoudt<sup>\*,†</sup>

Laboratories of Supramolecular Chemistry and Technology and Molecular Nanofabrication, MESA<sup>+</sup>  
Institute for Nanotechnology, University of Twente, P.O. Box 217, 7500 AE Enschede, The Netherlands,  
and Department of Chemistry and Institute of Chemistry and Biology of the Marine Environment,  
Carl von Ossietzky University of Oldenburg, PF 2503, D-26111 Oldenburg, Germany

Received June 2, 2006. In Final Form: August 4, 2006

Redox-active ferrocenyl (Fc)-functionalized poly(propyleneimine) (PPI) dendrimers solubilized in aqueous media by complexation of the Fc end groups with  $\beta$ -cyclodextrin ( $\beta$ CD) were immobilized at monolayers of  $\beta$ CD on glass ("molecular printboards") via multiple host–guest interactions. The directed immobilization of the third-generation dendrimer– $\beta$ CD assembly G3-PPI-(Fc)<sub>16</sub>-( $\beta$ CD)<sub>16</sub> at the printboard was achieved by supramolecular microcontact printing. The redox activity of the patterned dendrimers was mapped by scanning electrochemical microscopy (SECM) in the positive feedback mode using [IrCl<sub>6</sub>]<sup>3-</sup> as a mediator. Local oxidation of the Fc–dendrimers by the microelectrode-generated [IrCl<sub>6</sub>]<sup>2-</sup> resulted in an effective removal of the Fc–dendrimers from the host surface since the oxidation of Fc to the oxidized form (Fc<sup>+</sup>) leads to a concomitant loss of affinity for  $\beta$ CD. Thus, SECM provided a way not only to image the surface, but also to control the binding of the Fc-terminated dendrimers at the molecular printboard. Additionally, the electrochemical desorption process could be monitored in time as the dendrimer patterns were gradually erased upon multiple scans.

## Introduction

A key issue in molecular electronics,<sup>1</sup> sensors,<sup>2</sup> and biological arrays<sup>3</sup> is the positioning of molecules with high accuracy and stability on solid substrates. Most procedures to anchor molecules rely on physisorption, chemisorption, or covalent synthesis. Covalent synthesis does not allow rearrangement, self-correction, or intentional desorption. Chemisorption and physisorption do, but the thermodynamic and kinetic parameters are difficult to control. On the other hand, supramolecular interactions are specific, reversible, and tunable by multivalency and/or competitive agents, and a wealth of information on the binding strength and kinetics is readily available.<sup>4</sup> Therefore, our group has developed self-assembled monolayers (SAMs) consisting of receptor sites ("molecular printboards") to which molecules can bind via specific supramolecular interactions, allowing the binding of molecules with ultimate control over binding thermodynamics and kinetics. We have reported SAMs on gold of heptathioether-functionalized  $\beta$ -cyclodextrin ( $\beta$ CD), which forms well-ordered and densely packed monolayers.<sup>5</sup> Also, the synthesis and characterization of  $\beta$ CD SAMs at SiO<sub>2</sub> surfaces (i.e., glass slides

and oxidized silicon wafers) have been reported.<sup>6</sup> Various monovalent and multivalent guest molecules were positioned onto these SAMs by adsorption from solution and by using supramolecular microcontact printing ( $\mu$ CP) or dip-pen nanolithography with nanometer resolution.<sup>7–9</sup> Generally, supramolecular interactions are relatively weak, but using multivalent<sup>10</sup> guest molecules instead of monovalent guests increases the thermodynamic and kinetic stability of the adsorbed molecules at molecular printboards.

Dendrimers serve as a particularly suitable class of polyfunctional guest molecules since the number of end groups can be exactly controlled and all end groups are exposed at the periphery of the molecule.<sup>11</sup> Furthermore, the unique properties of dendrimers find applications in many fields such as drug delivery,<sup>12</sup> optoelectronics,<sup>13</sup> catalysis,<sup>14</sup> molecular recognition,<sup>15</sup>

\* To whom correspondence should be addressed. E-mail: b.j.ravoo@utwente.nl (B.J.R.), d.n.reinhoudt@utwente.nl (D.N.R.), gunther.wittstock@uni-oldenburg.de (G.W.).

<sup>†</sup> University of Twente.

<sup>‡</sup> Carl von Ossietzky University of Oldenburg.

(1) (a) Flood, A. H.; Stoddart, J. F.; Steuerman, D. W.; Heath, J. R. *Science* **2004**, *306*, 2055. (b) Service, R. F. *Science* **2001**, *294*, 2442. (c) Joachim, C.; Gimzewski, J. K.; Aviram, A. *Nature* **2000**, *408*, 541. (d) Tour, J. M. *Acc. Chem. Res.* **2000**, *33*, 791. (e) Gittens, D. I.; Bethell, D.; Schriffrin, D. J.; Nichols, R. J. *Nature* **2000**, *408*, 67. (f) Collier, C. P.; Mettersteig, G.; Wong, E. W.; Luo, Y.; Beverly, K.; Sampaio, J.; Raymo, F. M.; Stoddart, J. F.; Heath, J. R. *Science* **2000**, *289*, 1172.

(2) (a) Mehta, A. D.; Rief, M.; Spudich, J. A. *Science* **1999**, *283*, 1689. (b) Weiss, S. *Science* **1999**, *283*, 1676.

(3) (a) Nakamura, H.; Karube, I. *Anal. Bioanal. Chem.* **2003**, *377*, 446. (b) Pirrung, H. C. *Angew. Chem., Int. Ed.* **2002**, *41*, 1286. (c) Wilson, B. S.; Node, S. *Angew. Chem., Int. Ed.* **2003**, *42*, 494.

(4) Schneider, H. J.; Yatsimirsky, A. K. *Principles and Methods in Supramolecular Chemistry*; John Wiley & Sons Ltd.: Chichester, 2000.

(5) (a) Beulen, M. J. W.; Bügler, J.; Lammerink, B.; Geurts, F. A. J.; Biemond, E. M. E. F.; Leerdam, K. G. C.; Van Veggel, F. C. J. M.; Engbersen, J. F. J.; Reinhoudt, D. N. *Langmuir* **1998**, *14*, 6424. (b) Beulen, M. J. W.; Bügler, J.; De Jong, M. R.; Lammerink, B.; Huskens, J.; Schönherr, H.; Vancso, G. J.; Boukamp, B. A.; Wieder, H.; Offenhäuser, A.; Knoll, W.; Van Veggel, F. C. J. M.; Reinhoudt, D. N. *Chem.–Eur. J.* **2000**, *6*, 1176.

(6) Onclin, S.; Mulder, A.; Ravoo, B. J.; Huskens, J.; Reinhoudt, D. N. *Langmuir* **2004**, *20*, 5460.

(7) (a) Auletta, T.; Dordi, B.; Mulder, A.; Sartori, A.; Onclin, S.; Bruinink C. M.; Péter, M.; Nijhuis, C. A.; Beijleveld, H.; Schönherr, H.; Vancso, G. J.; Casnati, A.; Ungaro, R.; Ravoo, B. J.; Huskens, J.; Reinhoudt, D. N. *Angew. Chem., Int. Ed.* **2004**, *43*, 369. (b) Mulder, A.; Onclin, S.; Péter, M.; Hoogenboom, J. P.; Beijleveld, H.; ter Maat, J.; García-Parajó, M. F.; Ravoo, B. J.; Huskens, J.; van Hulst, N. F.; Reinhoudt, D. N. *Small* **2005**, *1*, 242.

(8) Onclin, S.; Huskens, J.; Ravoo, B. J.; Reinhoudt, D. N. *Small* **2005**, *1*, 852. (9) Bruinink, C. M.; Nijhuis, C. A.; Péter, M.; Dordi, B.; Crespo-Biel, O.; Auletta, T.; Mulder, A.; Schönherr, H.; Vancso, G. J.; Huskens, J.; Reinhoudt, D. N. *Chem.–Eur. J.* **2005**, *11*, 3988.

(10) Mammen, M.; Choi, S.-K.; Whitesides, G. M. *Angew. Chem., Int. Ed.* **1998**, *37*, 2754.

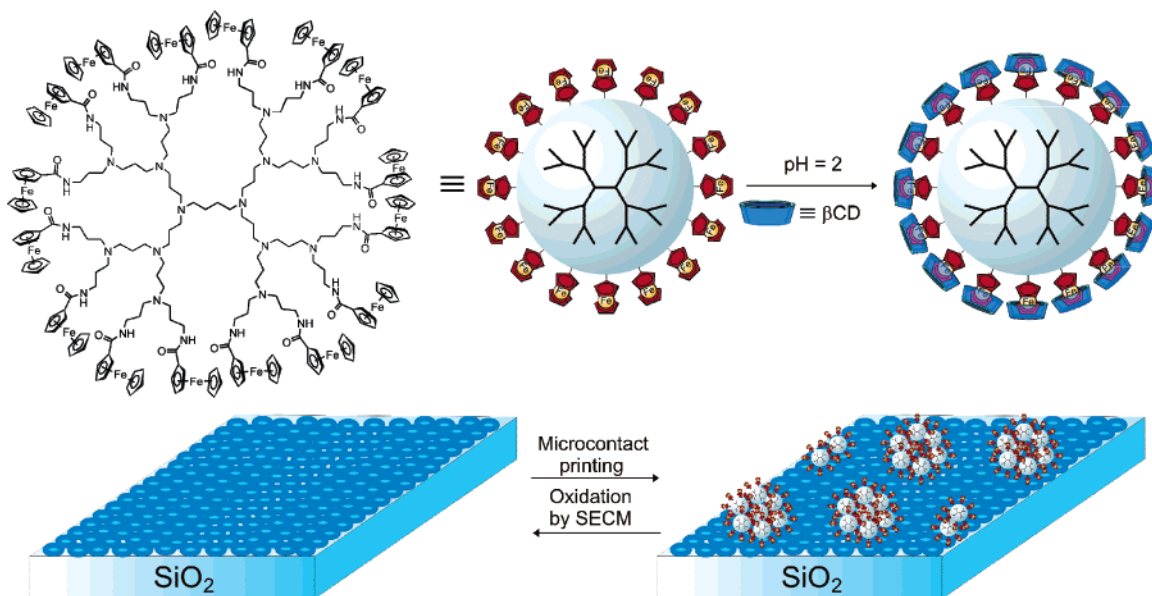
(11) (a) Tomalia, D. A. *Prog. Polym. Sci.* **2005**, *30*, 294. (b) Chase, P. A.; Klein Gebbink, R. J. M.; van Koten, G. J. *Organomet. Chem.* **2004**, *689*, 4016. (c) Bosman, A. W.; Janssen, H. M.; Meijer, E. W. *Chem. Rev.* **1999**, *99*, 1665.

(12) Boas, U.; Heegaard, M. H. *Chem. Soc. Rev.* **2004**, *33*, 43.

(13) Balzani, V.; Ceroni, P.; Maestri, M.; Vicinelli, C. S. V. *Top. Curr. Chem.* **2003**, *228*, 159.

(14) Twyman, L. J.; King, A. S. H.; Martin, I. K. *Chem. Soc. Rev.* **2002**, *31*, 69.

**Scheme 1. Complexation of G3-PPI-(Fc)<sub>16</sub> to  $\beta$ CD at pH 2, Resulting in Water-Soluble Dendrimer- $\beta$ CD Assemblies (Top), and Immobilization of the Fc-Dendrimer- $\beta$ CD Assemblies at the Molecular Printboard by  $\mu$ CP and Their Local Electrochemical Desorption by SECM (Bottom)**



and molecular encapsulation.<sup>16</sup> Recently, we reported the immobilization of adamantyl (Ad)-functionalized<sup>17</sup> and ferrocenyl (Fc)-functionalized<sup>18</sup> poly(propyleneimine) (PPI) dendrimer guest molecules at molecular printboards. Dendrimers of generation 1 up to generation 5 have 4, 8, 16, 32, or 64 end groups, respectively, and form multiple host-guest interactions with the molecular printboard. In the case of Fc-functionalized dendrimers, the precise number of Fc moieties that interact with the host surface was determined.<sup>18,19</sup> It is well-known that Fc is able to form inclusion complexes with  $\beta$ CD in aqueous media ( $K_a \approx 10^3 \text{ M}^{-1}$ ) and that the complexation is strongly diminished upon electrochemical conversion of the Fc groups to Fc<sup>+</sup> cations.<sup>20</sup> Consequently, the binding of the Fc-functionalized PPI dendrimers to the  $\beta$ CD SAMs on gold can be reversed electrochemically, even for a G5 PPI dendrimer with 64 Fc end groups having 7 or 8 host-guest interactions.<sup>18</sup>

So far, the binding control of these redox-active dendrimers has been limited to  $\beta$ CD SAMs at Au electrodes. However, applications in, for instance, nanofabrication require binding control not only at conducting surfaces, but also at nonconducting surfaces. Here we report the immobilization of Fc-dendrimers at molecular printboards on glass and the electrochemically induced desorption of the dendrimers from the host surface by scanning electrochemical microscopy (SECM). This work also represents a new SECM imaging technique where a monolayer of a surface-bound species is redox titrated by the SECM mediator. SECM allows electrochemical characterization or mapping of surfaces.<sup>21</sup> Due to the versatility and wide applicability of SECM for surface modification and functional characterization, it has

found applications such as measuring reaction rates of immobilized biomolecules<sup>22</sup> and following chemical processes in living cells<sup>23</sup> and in fundamental studies of charge-transfer processes at solid-liquid, liquid-liquid, and liquid-gas interfaces,<sup>24</sup> corrosion,<sup>25</sup> and electrocatalysis.<sup>26</sup> Almost all imaging applications were performed under steady-state conditions. Only very few studies are known where interfaces were probed by a redox compound until all the reactive material was exhausted,<sup>27</sup> although the significance of time-dependent information for kinetic studies has been emphasized recently by Unwin et al.<sup>28</sup>

## Results and Discussion

**Oxidation of Fc-Dendrimers.** The Fc-modified PPI dendrimers were prepared by condensation reactions of 1-(chloro-carbonyl)ferrocene with the terminal amino groups of the parent amino dendrimers according to a literature procedure.<sup>29</sup> The dendrimers are virtually insoluble in water, but in the presence

(15) (a) Daniel, M.-C.; Ruiz, J.; Nlate, S.; Blais, J.-C.; Astruc, D. *J. Am. Chem. Soc.* **2003**, *125*, 2617. (b) Ong, W.; Gomez-Kaifer, M.; Kaifer, A. E. *Chem. Commun.* **2004**, 1677.

(16) (a) Michels, J. J.; Huskens, J.; Reinhoudt, D. N. *J. Chem. Soc., Perkin Trans. 2* **2002**, 102. (b) Crooks, R. M.; Lemon III, B. I.; Sun, Lee L.; Yeung, K.; Zhao, M. *Top. Curr. Chem.* **2001**, *212*, 81.

(17) Huskens, J.; Deij, M. A.; Reinhoudt, D. N. *Angew. Chem., Int. Ed.* **2002**, *41*, 4467.

(18) (a) Nijhuis, C. A.; Huskens, J.; Reinhoudt, D. N. *J. Am. Chem. Soc.* **2004**, *126*, 12266. (b) Nijhuis, C. A.; Fu, Y.; Knoll, W.; Huskens, J.; Reinhoudt, D. N. *Langmuir* **2005**, *21*, 7866.

(19) Huskens, J.; Mulder, A.; Auletta, T.; Nijhuis, C. A.; Ludden, M. J. W.; Reinhoudt, D. N. *J. Am. Chem. Soc.* **2004**, *126*, 6784.

(20) Kaifer, A. E. *Acc. Chem. Res.* **1999**, *32*, 62.

(21) (a) Mandler, D. In *Scanning Electrochemical Microscopy*; Bard, A. J., Mirkin, M. V., Eds.; Marcel Dekker: New York, 2001; pp 593-627. (b) Shiku, H.; Uchida, I.; Matsue, T. *Langmuir* **1997**, *13*, 7239-7244. (c) Borgwarth, K.; Heinze, J. *J. Electrochem. Soc.* **1999**, *146*, 3285-3289. (d) Wilhelm, T.; Wittstock, G. *Electrochim. Acta* **2001**, *47*, 275-281. (e) Sauter, S.; Wittstock, G. *J. Solid State Electrochem.* **2001**, *5*, 205.

(22) (a) Zhao, C.; Sinha, J. K.; Wijayawardhana, C. A.; Wittstock, G. *J. Electroanal. Chem.* **2004**, *561*, 83. (b) Zhao, C.; Wittstock, G. *Anal. Chem.* **2004**, *76*, 3145-3154. (c) Wilhelm, T.; Wittstock, G. *Angew. Chem., Int. Ed.* **2003**, *42*, 2247. (d) Wittstock, G. *Fresenius' J. Anal. Chem.* **2001**, *370*, 303.

(23) (a) Bard, A. J.; Fan, F.-R. F.; Pierce, D. T.; Unwin, P. R.; Wipf, D. O.; Zhou, F. *Science* **1991**, *254*, 68. (b) Torisawa, Y.-S.; Kaa, T.; Takii Y.; Oyamatsu D.; Nishizawa M.; Matsue, T. *Anal. Chem.* **2003**, *75*, 2154. (c) Isik, S.; Etienne, M.; Oni, J.; Bloechl, A.; Reiter, S.; Schuhmann, W. *Anal. Chem.* **2004**, *76*, 6389. (d) Mauzeroll, J.; Bard, A. J.; Owhadian, O.; Monks, T. J. *Proc. Natl. Acad. Sci. U.S.A.* **2004**, *101*, 17587. (e) Holt, K. B.; Bard, A. J. *Biochemistry* **2005**, *44*, 13214.

(24) Barker, A. L.; Gonsalves, M.; Macpherson, J. V.; Slevin, C. J.; Unwin, P. R. *Anal. Chim. Acta* **1999**, *385*, 223.

(25) (a) Basame, S. B.; White, H. S. *J. Phys. Chem B* **1998**, *98*, 9812. (b) Zhu, Y.; Williams, D. E. *J. Electrochem. Soc.* **1997**, *144*, 43. (b) Still, J. W.; Wipf, D. O. *J. Electrochem. Soc.* **1997**, *144*, 2657.

(26) (a) Fernandez, J. L.; Walsh, D. A.; Bard, A. J. *J. Am. Chem. Soc.* **2005**, *127*, 357. (b) Shah, B. C.; Hillier, A. C. *J. Electrochem. Soc.* **2000**, *147*, 3043.

(27) Zhang, J.; Mandler, D.; Unwin, P. R. *Chem. Commun.* **2004**, 450-451.

(28) (a) Zhang, J.; Unwin, P. R. *Phys. Chem. Chem. Phys.* **2002**, *4*, 3814. (b) Barker, A. L.; Macpherson, J. V.; Slevin, C. J.; Unwin, P. R. *J. Phys. Chem. B* **1998**, *102*, 1586.

(29) Cuadro, I.; Morán, M.; Casado, C. M.; Alonso, B.; Lobete, F.; García, B.; Ibsate, M.; Losada, J. *Organometallics* **1996**, *15*, 5278.

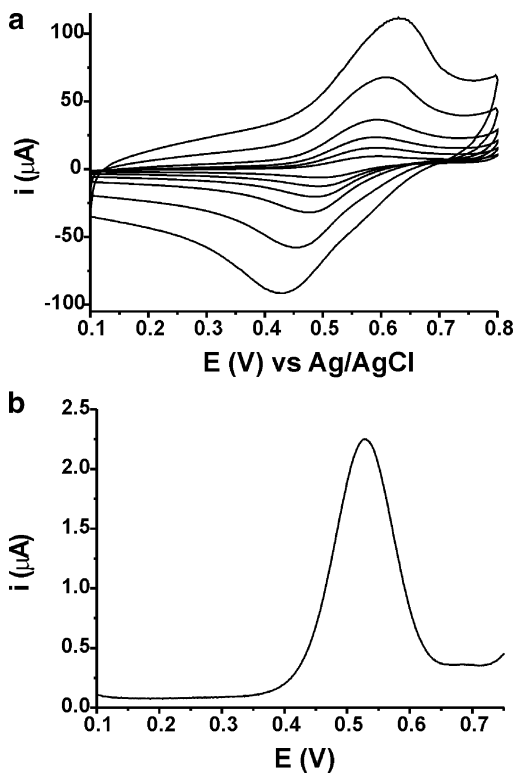


**Figure 1.** Cyclic voltammograms (A) at 10, 25, 50, 100, 250, and 500  $\text{mV s}^{-1}$  and differential pulse voltammogram (B) at 1  $\text{mV s}^{-1}$  of an aqueous solution of G3-PPI-(Fc)<sub>16</sub> complexed to  $\beta\text{CD}$  at pH 2 with 50 mM NaCl, using a bare Au working electrode.

of  $\beta\text{CD}$  ( $\beta\text{CD}/\text{Fc} = 1.1$ ) and at pH 2, all dendrimers could be solubilized in water after prolonged ultrasonication (Scheme 1). Under these conditions, the core amines are protonated and electrostatic repulsion forces the dendrimers into their most extended configuration. Therefore,  $\beta\text{CD}$  forms inclusion complexes with all Fc end groups, resulting in water-soluble multivalent dendrimer- $\beta\text{CD}$  assemblies (Scheme 1).

An aqueous solution of the Fc-dendrimer- $\beta\text{CD}$  assembly was characterized by cyclic voltammetry (CV) and differential pulse voltammetry (DPV) at bare Au electrodes (Figure 1). Cyclic voltammetry showed a single quasi-reversible oxidation wave at scan rates ( $\nu$ ) varying from 10 to 500  $\text{mV s}^{-1}$  (Figure 1A). The anodic peak potential  $E_{\text{p,a}}$  remains virtually unchanged. Only a scan rate of 500  $\text{mV s}^{-1}$  caused a shift of 20 mV to higher potentials compared to scan rates of 100  $\text{mV s}^{-1}$  or lower. In sharp contrast, the cathodic peak potential  $E_{\text{p,c}}$  was highly scan rate dependent and shifted almost 80 mV to lower potentials by increasing the scan rate from 10 to 500  $\text{mV s}^{-1}$ .

During oxidation all hydrophobic Fc- $\beta\text{CD}$  inclusion interactions are broken since neutral Fc moieties are converted to  $\text{Fc}^+$  cations, which do not form inclusion complexes with  $\beta\text{CD}$ .<sup>20</sup> Dissociation of the inclusion complex proceeds via a CE mechanism and is diffusion-independent.<sup>30</sup> Hence,  $E_{\text{p,a}}$  is constant, irrespective of the scan rate. On the other hand, during reduction,  $\text{Fc}^+$  is converted to Fc and the Fc- $\beta\text{CD}$  interactions are restored according to an EC mechanism. The  $E_{\text{p,c}}$  shifts to lower potential at higher scan rates since the Fc- $\beta\text{CD}$  association is diffusion-dependent. DPV also showed a single oxidation wave with the formal oxidation potential  $E^{\circ'}$  at 0.540 V vs Ag/AgCl, which was derived from  $E^{\circ'} = E_{\text{p}} - \Delta E/2$  (Figure 1B). These data prove that the interactions of the Fc groups on the dendrimer

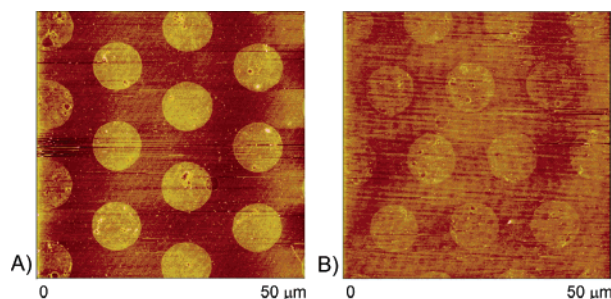


**Figure 2.** AFM images of the Fc-dendrimers printed on the molecular printboard on  $\text{SiO}_2$ : height images of printed patterns of G3-PPI-(Fc)<sub>16</sub> before rinsing (A) and after rinsing with water at pH 2 (B).

with  $\beta\text{CD}$  in solution can be electrochemically controlled. Furthermore, all redox centers are oxidized and reduced simultaneously and, thus, are electrochemically equivalent, indicating that all Fc moieties are complexed to  $\beta\text{CD}$  at pH 2. In contrast, Kaifer et al. found that aqueous solutions of G3-PPI-(Fc)<sub>16</sub>- $\beta\text{CD}$  assemblies at neutral pH showed two oxidation and reduction waves, which were attributed to complexed and uncomplexed Fc moieties.<sup>31</sup>

**Microcontact Printing of Fc-Dendrimers.** The G3-PPI-(Fc)<sub>16</sub>-( $\beta\text{CD}$ )<sub>16</sub> assemblies were immobilized in hexagonal patterns of dots (5  $\mu\text{m}$  in diameter and spaced by 3  $\mu\text{m}$ ) at the  $\beta\text{CD}$  host surface at  $\text{SiO}_2$  by supramolecular microcontact printing ( $\mu\text{CP}$ ).<sup>9</sup> In the contact areas, host-guest complexes are formed between the dendritic ink molecules and the  $\beta\text{CD}$  surface. We used G3-PPI-(Fc)<sub>16</sub>-( $\beta\text{CD}$ )<sub>16</sub> as ink molecules since according to previous work these dendrimers form kinetically stable assemblies at the host surface with on average four Fc- $\beta\text{CD}$  interactions per dendrimer.<sup>18</sup>

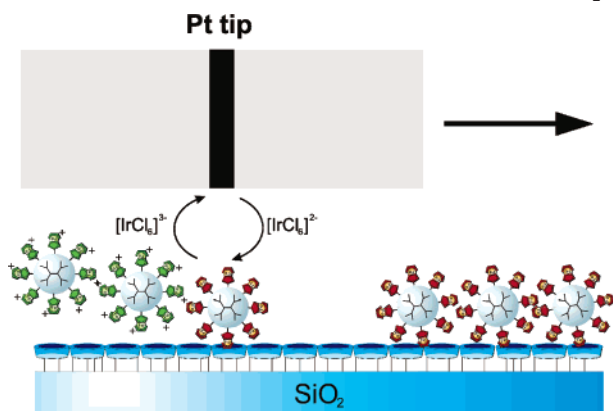
The patterns were characterized by AFM. The AFM images clearly show the transfer of dendrimers from the stamp to the substrate in patterns with a height of ca. 1 nm (Figure 2A). The stability of the patterns was verified by rinsing the patterns directly after printing with Millipore water at pH 2 (Figure 2B). Rinsing removes nonspecifically bound material to leave approximately a monolayer of dendrimers in the area of contact. Rinsing for prolonged periods of time did not result in removal of the dendrimers, indicating that the molecules form stable supramolecular assemblies at the  $\beta\text{CD}$  host surface at  $\text{SiO}_2$ . These observations are fully consistent with our earlier studies on guest dendrimers immobilized on the printboard from solution or by  $\mu\text{CP}$ .<sup>7-9,18</sup>

**Scanning Electrochemical Microscopy.** Patterns of G3-PPI-(Fc)<sub>16</sub> obtained by supramolecular  $\mu\text{CP}$  on the molecular printboard on  $\text{SiO}_2$  were also characterized by SECM. The SECM instrument used a disk-shaped Pt ultramicroelectrode (UME) of 25  $\mu\text{m}$  diameter. The dendrimers were printed in dots with a diameter of 50  $\mu\text{m}$  and gaps of 30  $\mu\text{m}$ , which are larger than the active electrode area of the UME, to ensure good resolution during imaging. The results were obtained by scanning the surface in aqueous solutions containing  $[\text{IrCl}_6]^{3-}$  as a mediator in the feedback mode. The UME potential  $E_{\text{T}}$  was kept at 0.75 V vs Ag/AgCl such that  $[\text{IrCl}_6]^{3-}$  is oxidized at the UME under diffusion-controlled conditions. The oxidized species  $[\text{IrCl}_6]^{2-}$  diffuses to the surface and may accept an electron from Fc moieties of the dendrimers, which have a lower  $E^{\circ'}$ . During this process,  $\text{Fc}^+$  would be released and  $[\text{IrCl}_6]^{3-}$  regenerated. Subsequently,  $[\text{IrCl}_6]^{3-}$  may diffuse back to the UME, giving rise to a positive

(30) Osella, D.; Carretta, A.; Nervi, C.; Ravera, M.; Gobetto, R. *Organometallics* **2000**, *19*, 2791.

(31) Castro, R.; Cuadrado, I.; Alonso, B.; Casado, C. M.; Morán, M.; Kaifer, A. E. *J. Am. Chem. Soc.* **1997**, *119*, 5760.

**Scheme 2. Mechanism of SECM-Induced Desorption of the Fc-Dendrimers from the Molecular Printboard on SiO<sub>2</sub><sup>a</sup>**



<sup>a</sup> [IrCl<sub>6</sub>]<sup>3-</sup> is oxidized at the tip and diffuses to the molecular printboard, where it oxidizes the patterns of G3-PPI-(Fc)<sub>16</sub> dendrimers. Subsequently, the oxidized dendrimers desorb from the host surface, and the reduced [IrCl<sub>6</sub>]<sup>3-</sup> diffuses back to the UME, giving rise to positive feedback currents only at the dendrimer-covered regions.

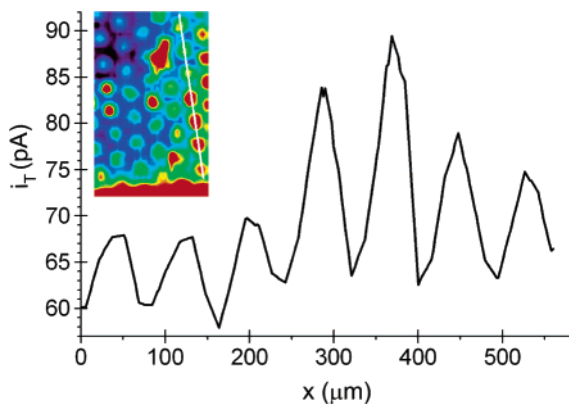


**Figure 3.** SECM image of the Fc-dendrimers printed on the molecular printboard on SiO<sub>2</sub> and line scan obtained from the profile of the image (inset) indicated by the white line in the image showing the periodicity of the printed features ( $E_T = 0.75$  V,  $v_T = 200$   $\mu\text{m s}^{-1}$ , 0.1 mM [IrCl<sub>6</sub>]<sup>3-</sup>).

feedback current. At locations where only a bare  $\beta$ CD monolayer is present, the [IrCl<sub>6</sub>]<sup>2-</sup> cannot be reduced, since no dendrimers are present, resulting in a UME current  $i_T$  that can be described by pure hindered diffusion of [IrCl<sub>6</sub>]<sup>3-</sup> from the solution bulk to the UME. The redox processes that occur are outlined in Scheme 2.

An SECM image is shown in Figure 3. The image clearly shows a hexagonal pattern of dots which appear with a higher feedback current compared to the background. The periodicity was determined from the profile of the image indicated by the white line, and the corresponding line scan is also shown in Figure 3. The observed periodicity of 80  $\mu\text{m}$  corresponds exactly to the printed dendrimer dots (50  $\mu\text{m}$  in diameter and 30  $\mu\text{m}$  gaps). Hence, SECM faithfully reveals the hexagonal pattern of a monolayer of dendrimers printed on the molecular printboard. The peak intensities of the line scan are not uniform, probably due to an inhomogeneous distribution of G3-PPI-(Fc)<sub>16</sub> at the surface.

To obtain the image in Figure 3, a very high scan rate and step size had to be used. The translation speed was 200  $\mu\text{m s}^{-1}$ , and the step size in the low-frequency axis ( $y$ ) was 15  $\mu\text{m}$ . At slower scan rates featureless images were obtained. We believe that this result was caused by the complete release of Fc-dendrimers

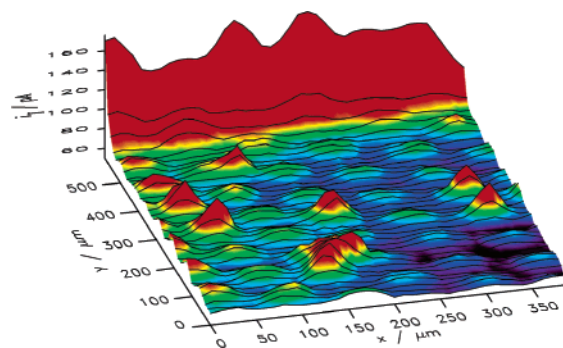


**Figure 4.** SECM image of a molecular printboard patterned with Fc-dendrimers illustrating the higher intensity of the first line scan (shown in the background) ( $E_T = 0.75$  V,  $v_T = 200$   $\mu\text{m s}^{-1}$ , 0.1 mM [IrCl<sub>6</sub>]<sup>3-</sup>). Black lines correspond to individual line scans. The false color was interpolated.

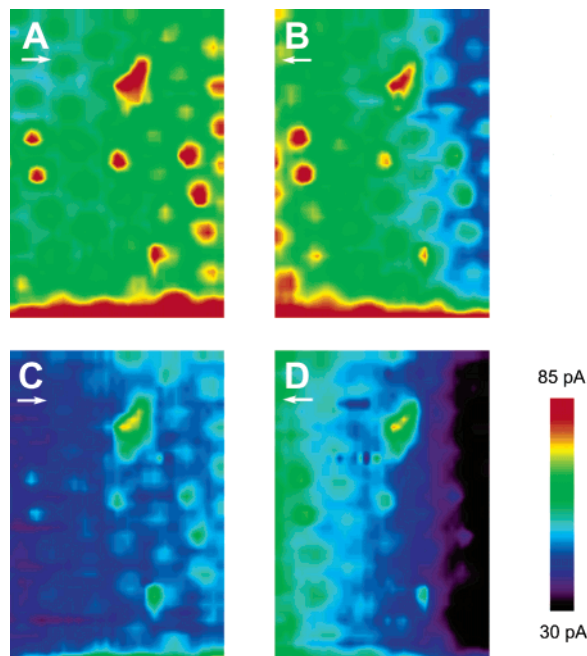


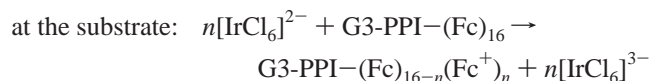
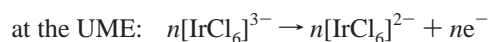
**Figure 5.** SECM images of G3-PPI-(Fc)<sub>16</sub> printed at a  $\beta$ CD SAM on SiO<sub>2</sub>: image composed of the (A) forward line scans and (B) backward line scans and a second SECM image of the same area composed of the forward line scans (C) and backward line scans (D) ( $E_T = 0.75$  V,  $v_T = 200$   $\mu\text{m s}^{-1}$ , 0.1 mM [IrCl<sub>6</sub>]<sup>3-</sup>).

during the scan, and mediator regeneration ceased before the current values were sampled. Even at higher scan rates the first line scans have the highest feedback current compared to the successive line scans in all obtained images. This is nicely demonstrated by the surface plot shown in Figure 4. Individual line scans are displayed as black lines and are recordings from subsequent forward scans. During the backward movement the same UME potential and translation rate were used. The first line scan is placed in the rear part of the plot. The first line scan is most intense because during the first line scan some of the Fc-dendrimers that are located in the area later probed by the UME are oxidized. In subsequent images, sample regions outside the imaging frame can contribute to the mediator regeneration, whereas the imaged region is successively depleted.

Upon imaging by SECM the feedback currents decreased significantly due to the depletion of Fc-loaded dendrimers on the surface. Moreover, repeated imaging of the same area showed a further decrease in feedback currents. Figure 5 shows four images of the same sample regions. The instrument allows the assembly of images from the forward line scans and the reverse

line scans. In this case, the same UME potential and translation rate were used for recording the images in the forward scan direction (Figure 5A,C) and the backward scan direction (Figure 5B,D). The sequence of recording is therefore first forward line scan of Figure 5A, first backward line scan of Figure 5B, second forward line scan of Figure 5A, second backward line scan of Figure 5B, and so on until the complete images in Figure 5A,B are recorded. The same process was repeated to obtain Figure 5C,D. The graphs are scaled to the same minimum and maximum and illustrate how the overall current and the contrast gradually fade from part A to part D of Figure 5. The features are hardly visible in the last image (Figure 5D).

The observations of (i) the relatively high intensity of the first line scan, (ii) the pattern disappearing upon scanning, and (iii) the high scan rate necessary to visualize the pattern all suggest that upon scanning the guest dendrimers desorb from the host surface. The proposed mechanism is outlined in Scheme 2. At the microelectrode the mediator is oxidized and diffuses to the surface where it may oxidize Fc groups of the dendrimers.<sup>32</sup> The reduced form of the mediator may diffuse back to the microelectrode. The oxidized form of Fc is not able to form inclusion complexes with the  $\beta$ CD at the surface, resulting in an effective desorption of the dendrimers from the surface. The reactions at the UME and at the substrate are thus



Therefore, subsequent scans and backward scans show a significant decrease in intensity of the feedback currents. The high scan rate is required to reduce the number of redox equivalents supplied per unit surface area, where it oxidizes the Fc units of the dendrimers. The dendrimers desorb from the host surface and diffuse into the bulk solution or oxidize neighboring dendrimers. Consequently, scanning slowly may supply more redox equivalents per unit sample surface area than Fc units present in the dendrimer-modified areas. For similar reasons the step size in the low-frequency direction was relatively large to minimize oxidation during scanning of the previous line scan. This also explains why the very first scan gives a substantially higher positive feedback current than the remaining line scans.

SECM-induced oxidation of the dendrimers resulted in an effective desorption of the dendrimers from the  $\beta$ CD SAM at  $\text{SiO}_2$  and also provided images of the desorption process at different stages by repetitively recording images until all Fc-dendrimers were desorbed. This observation implies that the dendrimers are primarily bound via specific host-guest interactions to the host surface on  $\text{SiO}_2$ . In principle, the monolayer is less ordered compared to monolayers on Au since the monolayer is covalently bound, but nevertheless, the binding behavior of the dendrimers is in full agreement with the studies of Fc-dendrimer binding to printboards on gold surfaces<sup>18</sup> and of divalent guest binding to printboards on glass.<sup>6,7</sup>

## Conclusions

SECM can electrochemically induce the desorption of Fc-dendrimers from a molecular printboard at  $\text{SiO}_2$ . The backward

scans showed a decrease in positive feedback currents compared to the forward scans, and imaging the same area a second time virtually removed all redox-active dendrimers from the host surface; thus, the desorption could be imaged at different stages. The reversible adsorption results from specific host-guest chemistry since Fc in the neutral form is able to form inclusion complexes with  $\beta$ CD while the oxidized cationic form is not.

The combination of supramolecular and electrochemical control of dendrimer adsorption is a promising tool in the integration of "bottom-up" and "top-down" nanofabrication schemes. For instance, local desorption of guest molecules by UME electrodes or smaller conductive AFM tips may give small template patterns exposing the molecular printboard to which other guest molecules may bind.

## Experimental Section

**Materials and Methods.** The Fc-terminated PPI dendrimers<sup>29</sup> and per-6-amino- $\beta$ -cyclodextrin<sup>33</sup> were synthesized according to literature procedures. All glassware used to prepare monolayers was immersed in piranha solution (concentrated  $\text{H}_2\text{SO}_4$  and 33%  $\text{H}_2\text{O}_2$  in a 3:1 ratio). *Warning: piranha solution should be handled with caution; it can detonate unexpectedly.* Next, the glassware was rinsed with large amounts of Milli-Q water. All adsorbate solutions were prepared prior to use. All solvents used in monolayer preparation were of p.a. grade.

**Substrate Preparation.** The synthesis of a  $\beta$ CD SAM on  $\text{SiO}_2$  substrates has been reported recently, and the same procedures was used here.<sup>6</sup> Microscope glass slides were activated by immersion in boiling piranha solution for 15 min, rinsed with copious amounts of Millipore water, and dried in a stream of  $\text{N}_2$ . Subsequently, a monolayer was formed by reaction with 1-cyano-11-(trichlorosilyl)-undecane. Reduction gave an amine-terminated monolayer which was converted to an isothiocyanate-terminated layer by reaction with 1,4-phenylene diisothiocyanate. Finally, reaction with per-6-amino- $\beta$ -cyclodextrin gave the host surface.

**Microcontact Printing.** The procedure for microcontact printing is very similar to that reported earlier for adamantyl-functionalized dendrimers.<sup>9</sup> Stamps were fabricated by casting a 10:1 (v/v) mixture of PDMS and curing agent (Sylgard 184, Dow Corning) against a photolithographically patterned silicon master and curing overnight at 60 °C. Subsequently, the stamps were peeled off the master and were mildly oxidized in a UV/ozone reactor for 60 min (Ultra-Violet Products Inc., model PR-100). Directly after oxidization the stamps were immersed in aqueous solutions containing the dendrimer- $\beta$ CD assemblies (1 mM in functionality and 1 mM  $\beta$ CD at pH 2). The stamps were inked for at least 20–30 min, and before printing the stamps were blown dry in a stream of  $\text{N}_2$ . The stamps were placed in conformal contact by hand with the host surface at  $\text{SiO}_2$  for 1 min without applying external pressure, after which the stamp was carefully removed. The substrates were used as such or rinsed with water at pH 2.

**Electrochemistry.** Electrochemical measurements were performed with an AUTOLAB PGSTAT10, in a custom-built three-electrode setup equipped with a platinum counter electrode, a Ag/AgCl reference electrode, and a screw cap holding the gold working electrode (area exposed to the solution 0.44  $\text{cm}^2$ ). CV spectra of the G3-PPI-(Fc)<sub>16</sub>- $\beta$ CD assemblies in aqueous solution (10 mM  $\beta$ CD at pH 2) with 50 mM NaCl were recorded at scan rates of 10, 25, 50, 100, 250, and 500  $\text{mV s}^{-1}$ . The DPV spectra were recorded using the same solution and a modulation time of 0.5 s, an interval time of 0.2 s, a step potential of 1 mV, and a modulation amplitude of 10 mV.

**SECM.** A home-built SECM instrument was used that consisted of a stepper motor positioning system (Märzhäuser, Wetzlar, Germany) and a CHI701B potentiostat used in a three-electrode configuration and operated via home-built software. The Pt UME

(32) The use of molecular printboards on nonconductive  $\text{SiO}_2$  substrates is advantageous for the SECM measurements because metal substrates (e.g., Au-thiol SAMs) may reduce the mediator by heterogeneous electron transfer, which complicates the data interpretation. See: Wittstock, G.; Schuhmann, W. *Anal. Chem.* **1997**, *69*, 5059–5066.

(33) Ashton, P. R.; Königer, R.; Stoddart, J. F.; Alker, D.; Harding, V. D. *J. Org. Chem.* **1996**, *61*, 903.

had a radius  $r_T = 12.5 \mu\text{m}$ , and  $\text{RG} = r_{\text{glass}}/r_T = 10$  ( $r_{\text{glass}}$  is the radius of the insulating glass shield). A Pt wire served as an auxiliary electrode and was used together with a Ag/AgCl reference electrode. The aqueous solution contained 0.1 mM  $\text{K}_3\text{IrCl}_6$  and 10 mM  $\text{KClO}_4$ . Initially the UME was positioned far from the surface and then approached the surface with the help of the SECM instrument by monitoring the steady-state  $\text{O}_2$  reduction current at  $E_T = -0.6 \text{ V}$  until the current stayed constant when the insulating sheath of the UME mechanically touched the sample surface. The UME was retracted  $10 \mu\text{m}$  from this point for horizontal scans. The sample tilt was minimized by scanning the UME horizontally over the surface several times while monitoring the steady-state  $\text{O}_2$  reduction current and adjusting the tilt table of the SECM instrument. The potential was then switched to  $E_T = 0.75 \text{ V}$  to oxidize  $[\text{IrCl}_6]^{3-}$  present in the solution. The translation speed of the UME across the surface

was maintained at  $200 \mu\text{m s}^{-1}$  with a step size of  $15 \mu\text{m}$  in the low-frequency scan axis.

**Acknowledgment.** The Dutch Technology Foundation STW is gratefully acknowledged for funding the Simon Stevin Award Project on Nanolithography (Grant No. TST4946 to D.N.R.). The work was partially funded by the Lower Saxony-Israeli Foundation (Grant No. ZN1744 to G.W.). Dr. Mária Péter obtained the AFM images shown in Figure 2. The contribution of Dr. Oleg Sklyar and Carolina Nunes Kirchner in constructing and programming the SECM instrument is gratefully acknowledged.

LA0615894